THEORETICAL NUCLEAR PHYSICS

DOE/ER/40335--4

DE89 015918

P. D. KUNZ

ERNEST ROST

JAMES R. SHEPARD

1989 PROGRESS REPORT

DISCLAIMER

CONTENTS

A. 1989 PROGRESS REPORT–October 1, 1988 to August 1, 1989

1. Dirac RPA Analysis of the Inelastic Scattering of 500 MeV Protons from ^{40}Ca E. Rost and J. R. Shepard

We have recently developed[1] a formalism and computer program for treating nuclear excitations using a non-spectral Dirac RPA approach. Such an approach is important in reaction calculations since it avoids expansion "in a box" intrinsic to the more common spectral approaches. The choice of 500 MeV proton scattering from a ^{40}Ca target is a particularly convenient case for study since the elastic scattering is well described in a Dirac framework, both phenomenologically and in impulse approximation. Finally data have recently been published[2] which measure analyzing powers and even a few spin-transfer quantities for strong inelastic scattering transitions.

The Random Phase Approximation (RPA) provides a framework for calculating collective 1p-1h excitations of doubly magic nuclei. As discussed in detail in Ref. 1, one derives an integral equation for the partial-wave polarization insertion, $\Pi^{ij;kl}_{LL'SS'J}$, which is solved in configuration space on a Gauss-Laguerre radial grid. Near the nth excited state, the polarization insertion behaves as a pole

$$\Pi^{ij;kl}(\vec{x},\vec{y};\omega \to \omega_n + \imath\eta) \longrightarrow -\frac{\left[\bar{\mathcal{F}}^{(n)}(\vec{x})\right]^{ij}\left[\mathcal{F}^{(n)}(\vec{y})\right]^{kl}}{\imath\eta}, \tag{1}$$

where $ij;kl$ are Dirac indices. After expanding in partial waves one can obtain the radial transition density

$$\left[\mathcal{F}^{(n)}_{LSJ}(x)\right]^{ij} = (-)^{i+j}\frac{\imath\eta}{\alpha}\left[\Pi^{ji;kl}_{LL'SS'J}(x,y_0;\omega_n+\imath\eta)\right]^* \tag{2}$$

with

$$\alpha^2 = (-)^{k+l+1}\imath\eta\Pi^{lk;kl}_{L'L'S'S'J}(y_0,y_0;\omega_n+\imath\eta). \tag{3}$$

In the numerical calculation, a small value of η (typically 0.1 MeV) is used and the resulting $\mathcal{F}$ extracted is almost purely real and independent of η.

For the natural parity transitions considered in this work $[L,S]$ takes on the values $[J,0]$, $[J,1]$, $[J-1,1]$, and $[J+1,1]$. For the first two cases the ij indices must be the same; for the last two cases, the ij indices are different. Thus the extracted $\mathcal{F}^{ls}$ give the eight radial transition densities appropriate for the target space parts of the DWIA calculation outlined in Ref. 3. We note that the $[J,0]$ densities enter in the (e,e′) *Coulomb* form factor while the others contribute to

the electric form factor. We refer to the latter generically as $\Delta S = 1$ terms. It should be noted that the $\Delta S = 1$ terms do not appear in collective model calculations of (p,p′) where transition densities are constructed by deforming the optical potential.

Calculations were performed for the lowest 3^- and 5^- levels in ^{40}Ca known to be at excitation energies of 3.74 MeV and 4.49 MeV, respectively. Comparison with the data of Lisantti *et al.*[2] is made in Figs. 1 and 2 for the 3^- excitation by the (p,p′) reaction at 500 MeV. The theoretical calculation has not been renormalized, *i.e.,* no additional collectivity beyond the RPA is indicated. A similar result occurs in electron scattering where the RPA calculation agrees with experimental[4] Coulomb form factor data. The dashed curves in the figure show the effect of omitting all $\Delta S = 1$ terms as would occur in a collective model treatment—these curves are actually quite close to those obtained in a collective model calculation where the optical model densities are deformed. Finally a pure shell-model particle-hole calculation is shown to demonstrate the large collectivity. It should be emphasized that all these calculations employ the same distortion and interaction so that only nuclear structure effects are being compared.

Inspection of Figs. 1 and 2 shows that the gross features of the (p,p′) reaction are adequately described by the theory (except for the obvious lack of collectivity in the single-particle description.) However, there are small differences between the calculations for the spin-dependent observables and the RPA-model approach appears to give an overall better description of the data for this particularly favorable case.

Calculations for the excitation of the lowest 5^- level in ^{40}Ca by 500 MeV protons are shown in Fig. 3. In this case the collectivity is less and the RPA calculations now underestimate the data by a factor ~ 1.6 near the peak. A similar underestimation was found when our RPA calculation was compared with experimental (e,e′) data[4]. Also the several A_y curves do not differ as much as for the 3^- case, although here the agreement with the existing data is good. It would be interesting to have more spin-observable data, especially spin-transfer quantities, since they would be more useful in testing nuclear structure models.

We have found that a simple but fully microscopic relativistic mean-field-theory + RPA can describe elastic *and* strong inelastic scattering of 500 MeV protons from ^{40}Ca. For the inelastic cases our RPA treatment provides $\Delta S = 1$ terms which contribute, *e.g.,* to transverse electron scattering terms and which do not occur in conventional collective model (p,p′) calculations. The limited (p,p′) spin observable data available are somewhat better described with our RPA approach. We take these results as further evidence that QHD1-MFT and its RPA extension provide an internally consistent model of nuclear structure and scattering which accurately describes numerous physical quantities with *very* few free parameters.

1. J.R.Shepard, E.Rost, and J.A.McNeil, Phys. Rev C (to be published; *ibid.*, Univ. of Colorado report NPL 1044, pg. 123 (1988)
2. J.Lisantti *et al.*, Phys. Rev. **C39**, 538 (1989)
3. J.R.Shepard, E.Rost, and J.Piekarewicz, Phys. Rev. **C30**, 1604 (1984)
4. J.Heisenberg *et al.*, Nucl. Phys. **A164**, 353 (1971); P.L.Hallowell *et al.*, Phys. Rev. **C7**, 1396 (1973)

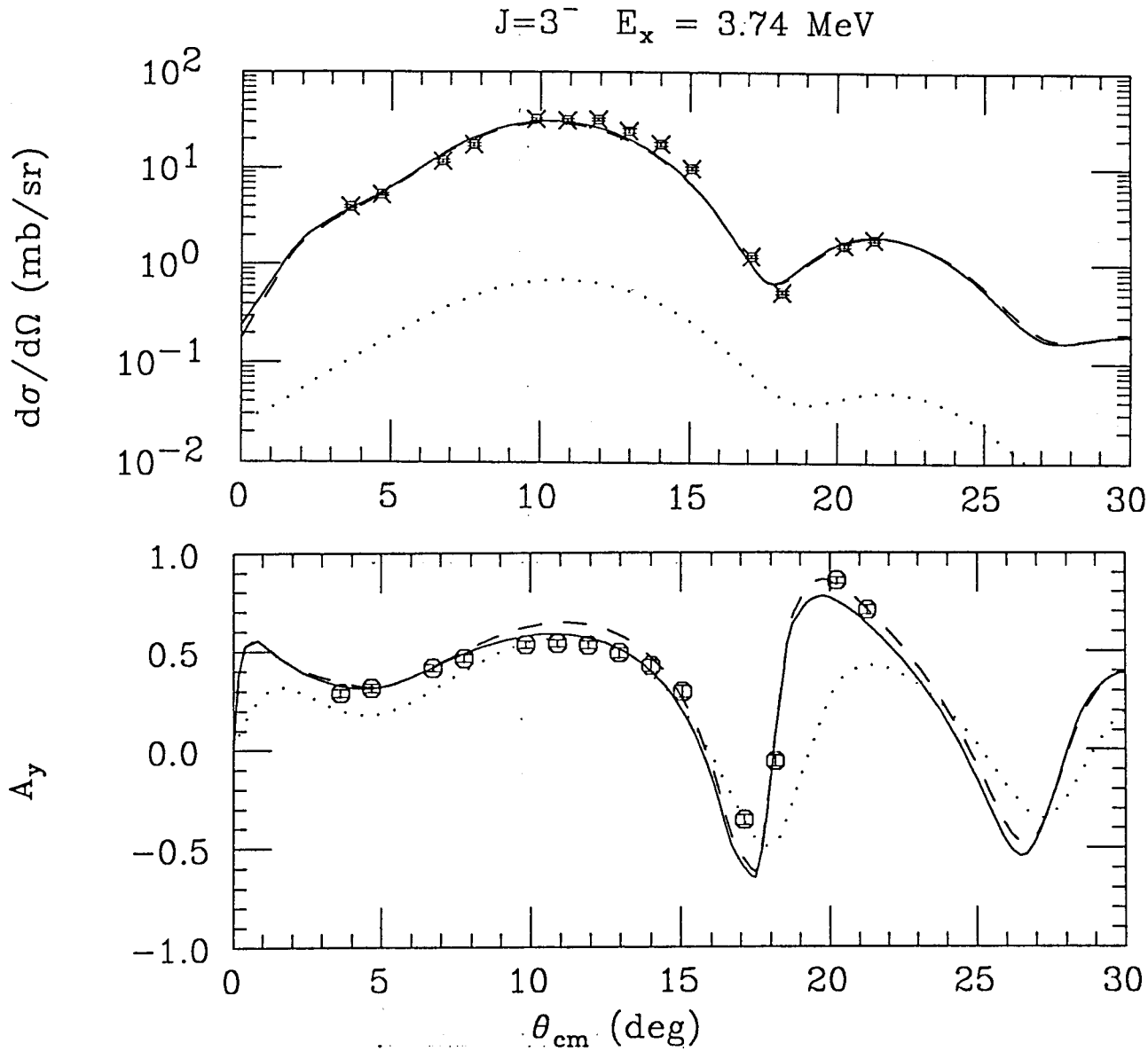

Fig. 1. Experimental and theoretical cross sections and analyzing powers for the excitation of the 3.74 MeV 3^- level of ^{40}Ca by 500 MeV protons. The data are taken from ref. 2. The solid curve is obtained from a relativistic impulse approximation calculation using non-spectral transition densities F. The dashed curve is obtained using only $\Delta S = 0$ terms and is very close to a collective model calculation with a deformed optical potential. The dotted calculation is the result of a transition involving a single particle $d_{3/2} \rightarrow f_{7/2}$ transition.

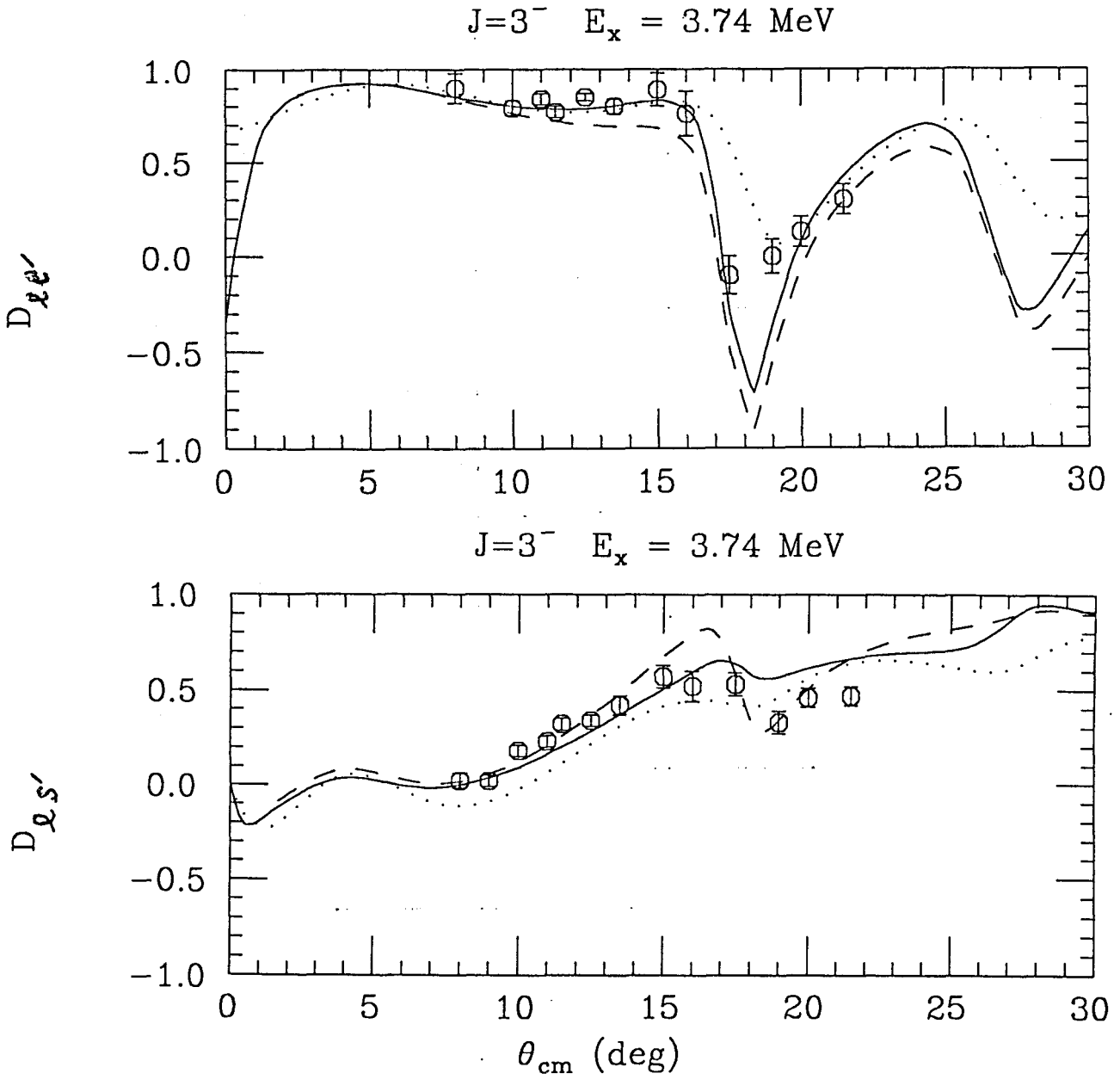

Fig. 2. Experimental and theoretical spin-transfer coefficients for the excitation of the 3.74 MeV 3^- level of ^{40}Ca by 500 MeV protons. The data are taken from ref. 2. The theoretical curves are described in the caption to Fig. 1.

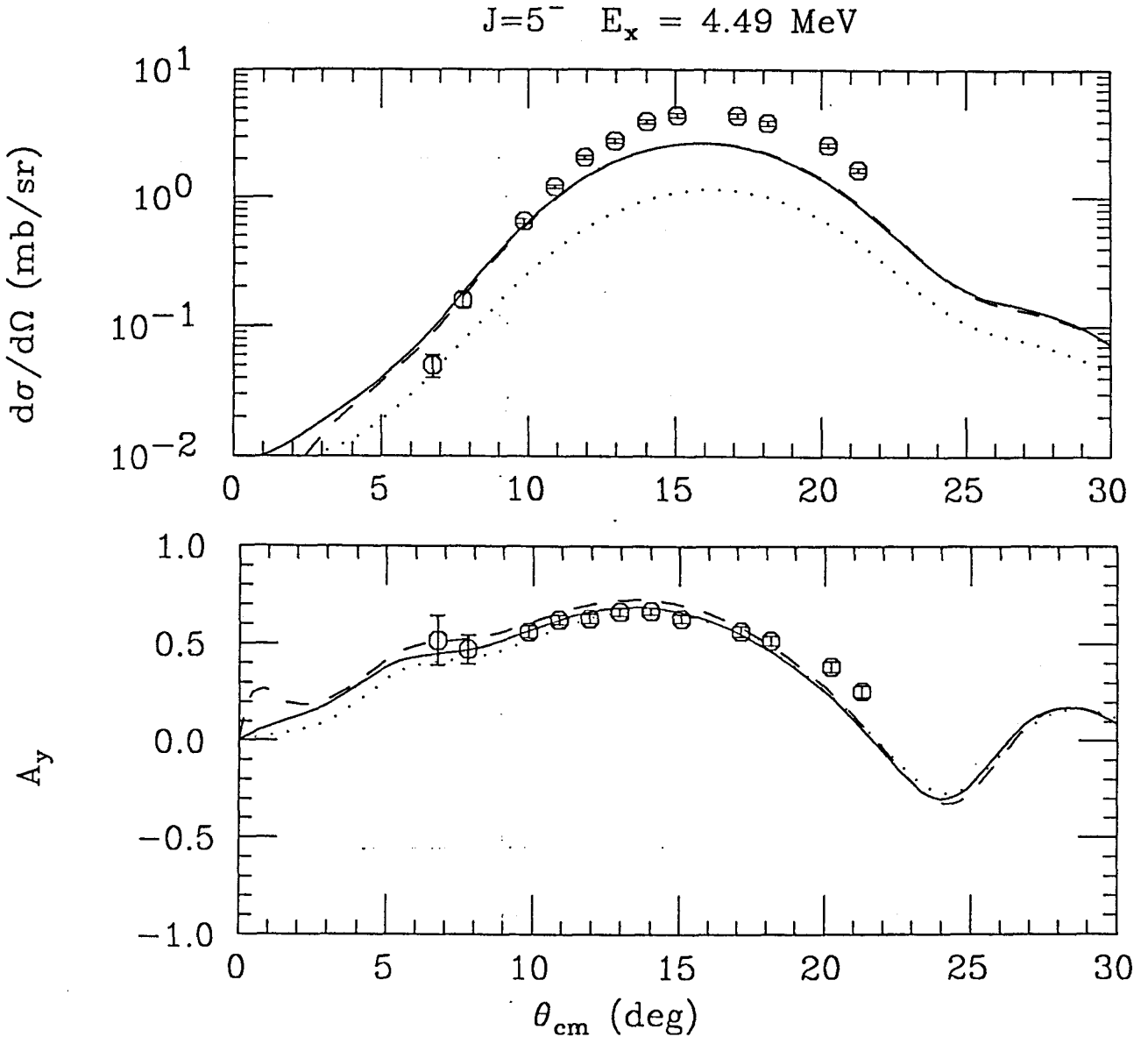

Fig. 3. Experimental and theoretical cross sections and analyzing powers for the excitation of the 4.49 MeV 5^- level of ^{40}Ca by 500 MeV protons. The data are taken from ref. 2. The theoretical curves are described in the caption to Fig. 1.

2. **Giant resonances at complex excitation energies** J. R. Shepard, D. S. Oakley, R. J. Peterson and E. Rost

Collective excitations are familiar nuclear phenomena. Strong, low-lying quadrupole and octupole excitations are observed in nearly all nuclei and such excitations are well-described by microscopic many-body theories such as the random-phase-approximation (RPA). Similar collective phenomena are seen in the nuclear continuum in the form of giant resonances which appear in experimental spectra as broad and systematic features above some smoother background. Continuum excitations pose special problems both experimentally and theoretically. In particular, for continuum calculations, various resonances overlap and a smooth background is present which does not allow, in any obvious way, the useful factorization possible in the discrete case. This means that it is not obvious even how precisely to define a giant resonance; for example, we can not readily identify its transition density in the same way as for a discrete excitation. In fundamental scattering theory resonances are often defined in terms of the behaviour of the scattering matrix in the complex plane although this approach is not usually employed in microscopic many-body theories.

We have examined the continuum RPA p-h propagator (or polarization insertion) for ^{40}Ca based on a relativistic (QHD-1) mean-field-theory (MFT) ground-state. The p-h propagator is evaluated for *complex* excitation energies, ω, and giant resonance contributions to the nuclear response are identified with poles in the p-h propagator in the complex ω-plane. This picture provides a clear theoretical working definition of what a giant resonance is and permits direct extraction of a transition density for the giant resonance even when continuum effects contributing to the escape width are included. Although the calculations to be described below are based on a relativistic model of nuclear structure, the points we wish to stress are quite general and apply to any continuum-RPA treatment.

QHD-1[1] is a relativistic field-theoretic model of nuclear dynamics based on the interaction of a nucleon field with an attractive scalar-isoscalar σ-meson field and a repulsive vector-isoscalar ω-meson field. The mean-field approximation in this model provides a good description of the properties of the ground states of doubly-magic nuclei with few free parameters. A random-phase-approximation (RPA) calculation based on this mean-field-theory (MFT) has recently been developed and has proven to be successful for the description of 1p-1h excitations in doubly-magic nuclei . A variety of numerical techniques have been employed to solve the QHD-1 RPA and we now focus on the so-called "non-spectral" method[2] in which the correct continuum boundary conditions may straightforwardly be included.

The RPA is embodied in the schematic integral relation

$$\Pi_{RPA} = \Pi_{MF} + \Pi_{MF}\ K\ \Pi_{RPA}, \tag{1}$$

where Π_{RPA} is the correlated RPA particle-hole propagator and K is the interaction kernel which depends on the meson masses and meson-nucleon-nucleon

coupling constants. In Ref. 2, the integral form of the RPA equation is solved directly and low-lying discrete excitations are identified as singularities in Π_{RPA} at $\omega = \omega_n$, real. The residues at these poles are obtained numerically and the associated RPA transition density $\mathcal{F}^{(n)}$ can then be extracted. The transition densities then yield matrix elements of one-body operators and observables for processes like inelastic electron scattering. Comparison of excitation energies and electron-scattering form factors computed in large-basis spectral RPA calculations[3] with calculations using the non-spectral method[2] shows that the two methods are essentially equivalent for discrete excitations.

The linear response of a nucleus to a probe whose interaction vertex with a nucleon is represented by the operator $\mathcal{O}$ is expressed quite generally in terms of Π_{RPA} via

$$S_{\mathcal{O}}(\omega) = -\frac{1}{\pi}\text{Im Tr}[\mathcal{O}\Pi_{RPA}(\omega)\mathcal{O}]. \tag{2}$$

An accurate calculation of this expression is very difficult because of the complicated structure of O (involving, e.g., the NN t-matrix and distorted waves.) However, we will outline a method—generalizing from resonant single-particle levels in the mean field approach—which will allow us to properly include continuum effects and yet retain the simplicities associated with discrete excitations.

It is well known[4], that the single-particle (or mean-field) propagator will have poles at *complex* ω below the real axis which correspond to resonant single-particle levels. If we express the position of such a pole as $\epsilon_\alpha - i\Gamma_\alpha/2$, the width of the resonance is given by Γ_α. We now recall that Π_{MF} has poles at $\epsilon_\alpha - \epsilon_\beta$ where $\epsilon_\alpha(\epsilon_\beta)$ is the eigenenergy of the particle (hole) single particle state. If Π_{MF} is computed using the spectral method, and if α labels a *resonant* single particle state, Π_{MF} will have a pole at a complex frequency, $\omega_{\alpha\beta} = \epsilon_\alpha - \epsilon_\beta - i\Gamma_\alpha/2$. The response defined using the MFT analogue of Eq. (2) will contain a contribution due to the pole at $\omega_{\alpha\beta}$ given by

$$\begin{aligned} S^{\alpha\beta}_{\mathcal{O}}(\omega) &= |\ \langle\mathcal{O}\rangle_{\alpha\beta}\ |^2 \cdot(-\frac{1}{\pi})\text{Im}\left[\frac{1}{\omega - \omega_{\alpha\beta}}\right] \\ &= |\ \langle\mathcal{O}\rangle_{\alpha\beta}\ |^2\ \frac{\Gamma_\alpha/2\pi}{\omega^2 - (\epsilon_\alpha - \epsilon_\beta)^2}, \end{aligned} \tag{3}$$

where $\langle\mathcal{O}\rangle_{\alpha\beta} = \text{Tr}[\mathcal{O}\mathcal{F}_{\alpha\beta}]$ and $\mathcal{F}_{\alpha\beta}$ is the single particle transition density[3]. Thus this partial response looks just like the usual discrete response except for an additional Breit-Wigner distribution of strength. The discrete case is, of course, recovered in the limit $\Gamma_\alpha \to 0$.

We anticipate that the analytic behaviour described above will persist when RPA correlations are included but that the pole positions and residues of Π_{RPA} will differ from those of Π_{MF}. More specifically, we expect that giant resonances will appear as poles in Π_{RPA} with particularly large residues just as RPA correlations concentrate transition strength in low-lying discrete collective levels.

To investigate this question we have evaluated the non-spectral isoscalar quadrupole QHD-1 MFT RPA particle-hole propagator for ^{40}Ca using the calculational methods outlined in Ref. 2. This RPA propagator was evaluated at a grid of points in the complex ω-plane in the region $10 \leq \mathrm{Re}\ \omega \leq 35$ MeV and $0.1 \leq -\mathrm{Im}\omega \leq 7$ MeV. In Fig. 1 we show a 3-dimensional plot of the quantity

$$S_{\mathcal{O}}(\mathrm{Re}[\omega]) \sim \left|\Pi^{11;11}_{RPA;J=2^+,T=0}(x_0, x_0; \omega)\right| / \mathrm{Im}\ \omega, \tag{4}$$

where 11;11 denotes upper Dirac indices and where x_0 is a matching radius roughly corresponding to the radius of the nucleus. This plotted quantity is convenient calculationally and is approximately proportional to the contribution of $\Pi_{RPA}(\omega)$ to the giant resonance response at its peak.

As is evident from Fig. 1 $S_{\mathcal{O}}$ is highly structured with sharp peaks at points in the ω-plane. We identify each of the peaks as a numerical approximation to poles in Π_{RPA} which in turn we associate with individual components of the isoscalar quadrupole giant resonance. This association is established by examining the isoscalar component of the ^{40}Ca response. which should consist of peaks corresponding to the structures seen in Fig. 1 and having widths given by the distance of these structures from the real axis. These resonant contributions ride on a non-resonant background without sharp structure in the complex ω-plane.

The appropriateness of our resonance interpretation is indicated in Fig. 2 where a decomposition of the computed ΔT=0 response in terms of Breit-Wigner peaks riding on a smooth background has been made. This decomposition assumes the Breit-Wigner shapes to have centroids and widths corresponding to the complex ω values of the resonant structures shown in Fig. 1. The overall strength of each peak in the response was determined by a best-fit procedure. Figure 2 shows that this decomposition gives an excellent reproduction of the full response. Furthermore, the response of each peak, as determined by the fitting coincides very well with the numerically determined *residue* of the corresponding singularity in the quantity defined in Eq. (4) and displayed in Fig. 1. This leads to a working definition of a giant resonance as a singularity of the particle-hole propagator with a large residue which is analogous to an ordinary discrete collective excitation in every way except that the singularity appears at a complex frequency rather than a real one. Furthermore, the imaginary part of the pole position corresponds to the escape width of the resonance. While RPA correlations shift the energy and alter the strength of simple particle-hole (or MFT) discrete excitations, they may also affect the *width* of resonances by shifting their poles vertically in the complex ω-plane.

Similar calculations and plots for the uncorrelated (or MFT) analogue of the RPA calculation and plots yield structures quite different from those shown in Fig. 1. The most striking difference is the very strong peak in the RPA calculation at $\omega = 22.3 - i0.83$MeV which gives the dominant contribution to the response in Fig. 2 and should perhaps be considered *the* isoscalar quadrupole giant resonance. Our numerical methods allow for the extraction of transition densities for the giant resonance with continuum effects automatically included. Preliminary comparisons with data are encouraging.

1. B.D.Serot and J.D.Walecka, Adv. Nucl. Phys. **16**, 1 (1986)
2. J.R.Shepard, E.Rost, and J.A.McNeil, Phys. Rev C (to be published; *ibid.*, Univ. of Colorado report NPL 1044, pg. 123 (1988)
3. R.J.Furnstahl, Phys. Lett. **152B**. 313 (1985); R.J. Furnstahl contribution to "Int. Conf. on Spin Observables of Nuclear Probes," Telluride, CO, Plenum (N.Y.) 1989
4. see, e.g., J.R.Taylor, *Scattering Theory: The Quantum Theory of Nonrelativistic Collisions*, R.E.Kreiger, Malabar FL (1983)

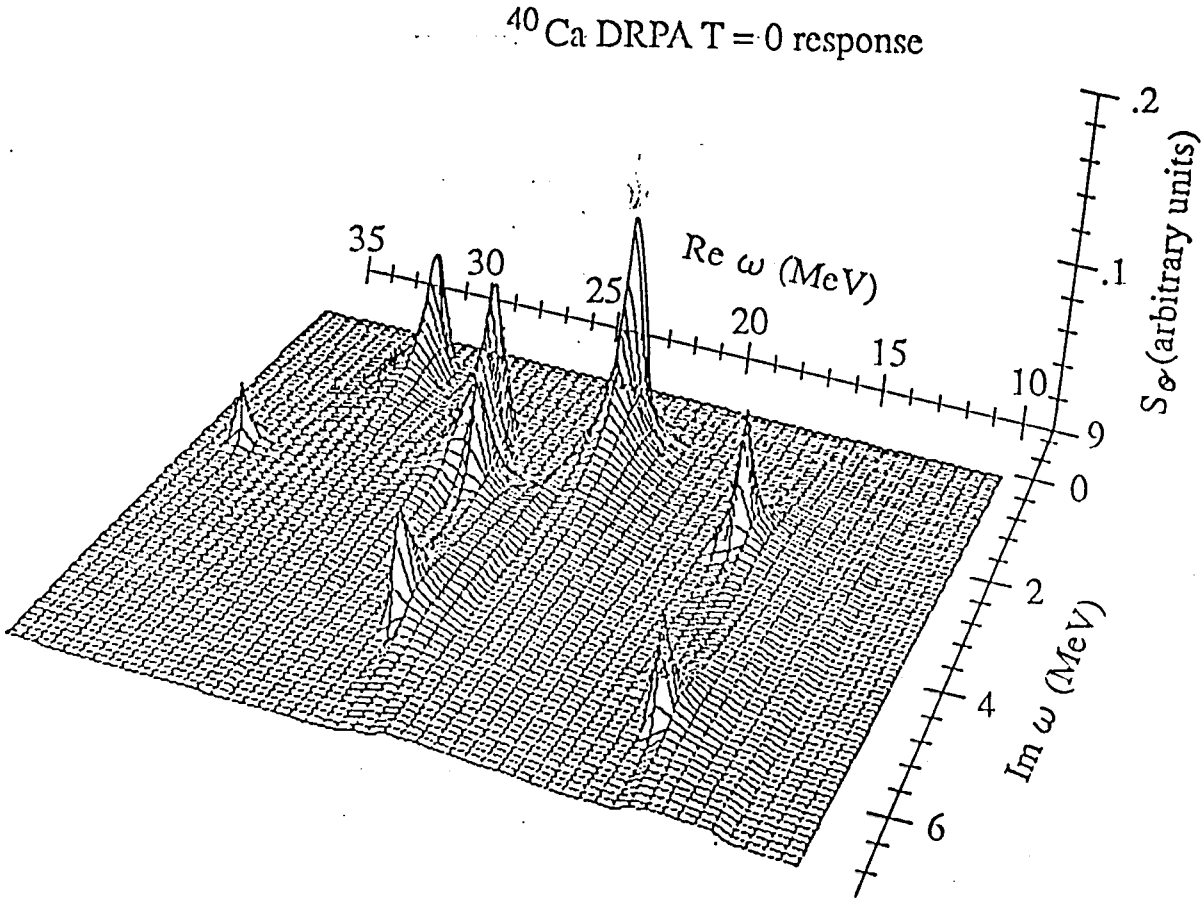

Fig. 1. ^{40}Ca T=0, L=2^+ RPA response in the complex ω plane.

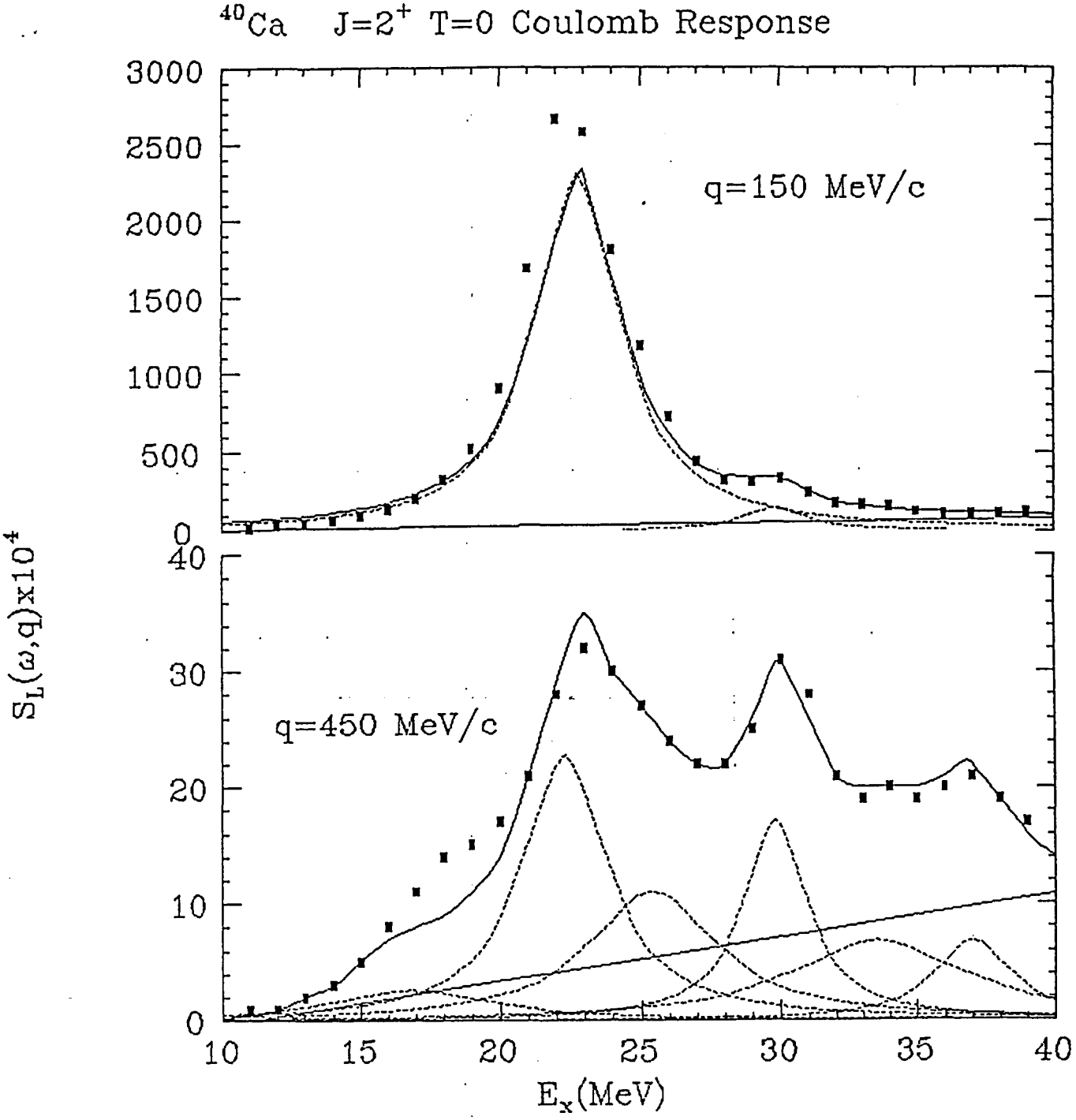

Fig. 2. Peak fitting analysis of the 2^+ RPA response versus excitation energy at momentum transfers of 150 and 450 MeV/c. The points represent an "exact"calculation using Eq. 2; the dotted lines are the fitted curves using the positions and widths of the poles displayed in Fig 1. The solid line is the sum of the several pole contributions.

3. Analysis of the $0^+ \rightarrow 0^-$ inelastic scattering reaction at intermediate energies E. Rost

The $0^+ \rightarrow 0^-$ transition by medium-energy proton inelastic scattering is a potentially rich source of new nuclear structure information. A general inelastic scattering reaction requires[1] three nuclear structure densities: the spin-independent longitudinal density ρ, the spin-dependent transverse density Σ_T, and the spin-dependent longitudinal density Σ_L. For a $0^+ \rightarrow 0^-$ transition only the last term is non-zero and hence can be studied in isolation from the other, generally larger, terms. In a relativistic model similar simplicities obtain[2], where now the usually dominant σ- and timelike ω- meson terms vanish allowing for the study of smaller, exotic parts of the t-matrix.

A most favorable case would appear to be the 0^- level in ^{16}O at 10.957 MeV since it should have a simple $p^{-1}_{1/2}s_{1/2}$ $T = 0$ structure. Unfortunately experiments at intermediate energies (where an impulse approximation analysis can be used) are difficult since this level is weak and is only 0.14 MeV separated from strong natural parity levels. Nevertheless some (p,p′) data exist[3] and, although tentative, do give a suggestion that the simple reaction and/or nuclear structure models may be inadequate for this case.

The theoretical calculations presented in the figures employ a microscopic relativistic treatment[5] of the inelastic scattering reaction. A distorted wave impulse approximation is used where the transition amplitude driving the reaction is obtained from NN scattering data. The comparison of these calculations with the data is given by the solid curves in the figure and is seen to be marginal at best. These calculations treat nucleon exchange only implicitely (in the sense that exchange effects are not separated in the fit NN amplitudes.) When exchange is included implicitely, the agreement with data is *not* improved—also, similar discrepancies appear in non-relativistic treatments[1] and in a careful alternative relativistic calculation[6].

Of particular interest is the recent preliminary forward angle analyzing power data at 400 MeV which is seen to be *negative* with $A_y \sim -1$ for the 4.4° point. Such a descrepancy is hard to understand with any reasonable (and even unreasonable) changes in distortion or interaction. Indeed the only way I was able to obtain a large negative analyzing power at forward angles was to invoke considerable isospin mixing. In the figures are shown the extreme case where the level is treated as a pure-proton or pure-neutron excitation. The pure-proton case is seen to give a negative analyzing power at forward angles with comparable fits to the other data. If these data are verified (improved experiments are expected in the next few months), then it will be appropriate to examine the isospin mixing as well as other effects to try to understand this simple, yet baffling, reaction.

1. W.G.Love *et al.*, in *Proceedings of International Conference on Spin Excitations*, Telluride, CO, edited by F. Petrovich *et al.* (1982); S.S.M.Wong *et al.*, Phys. Lett. **149B** 299 (1984)
2. J.R.Shepard, E.Rost, and J.McNeil, Phys. Rev. **C33**, 634 (1986)
3. J.J.Kelly, Ph.D Thesis, M.I.T. 1981 (unpublished)
4. J.King, private communication
5. J.R.Shepard, E.Rost and J.Piekarewicz, Phys. Rev. **C30**, 1604 (1984)
6. J.Piekarewicz, Phys. Rev. **C35**, 675 (1987)

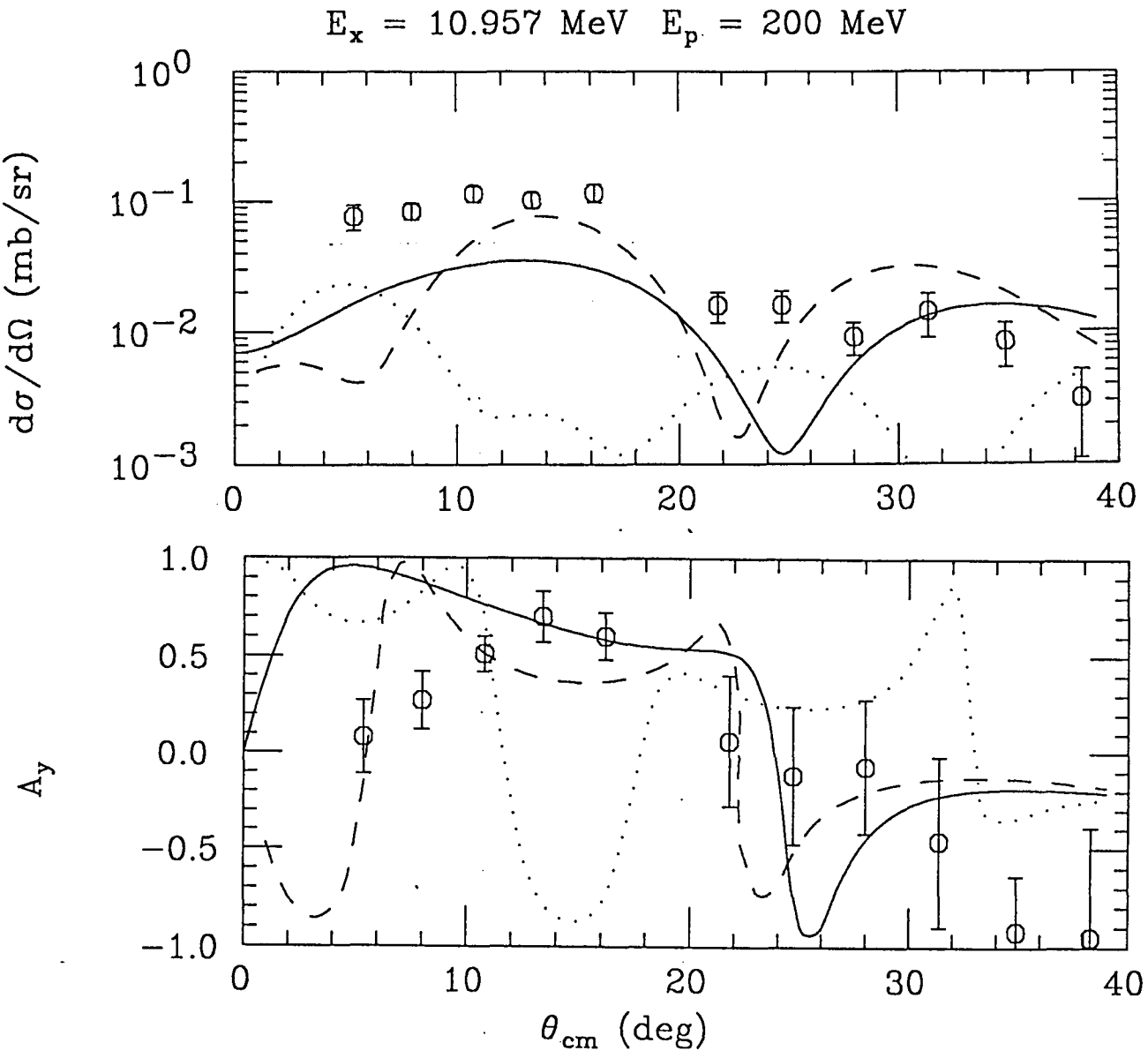

Fig. 1. Experimental and theoretical cross sections and analyzing powers for the excitation of the 10.957 MeV 0^- level of ^{16}O by 200 MeV protons. The data are taken from ref. 4. The solid curve is obtained from a relativistic impulse approximation calculation treating the 0^- state as a pure T=0 level. The dashed cureve is a similar caclulation assuming a pure proton $p^{-1}_{1/2}s_{1/2}$ excitation and the dotted curve uses a pure neutron excitation assumption.

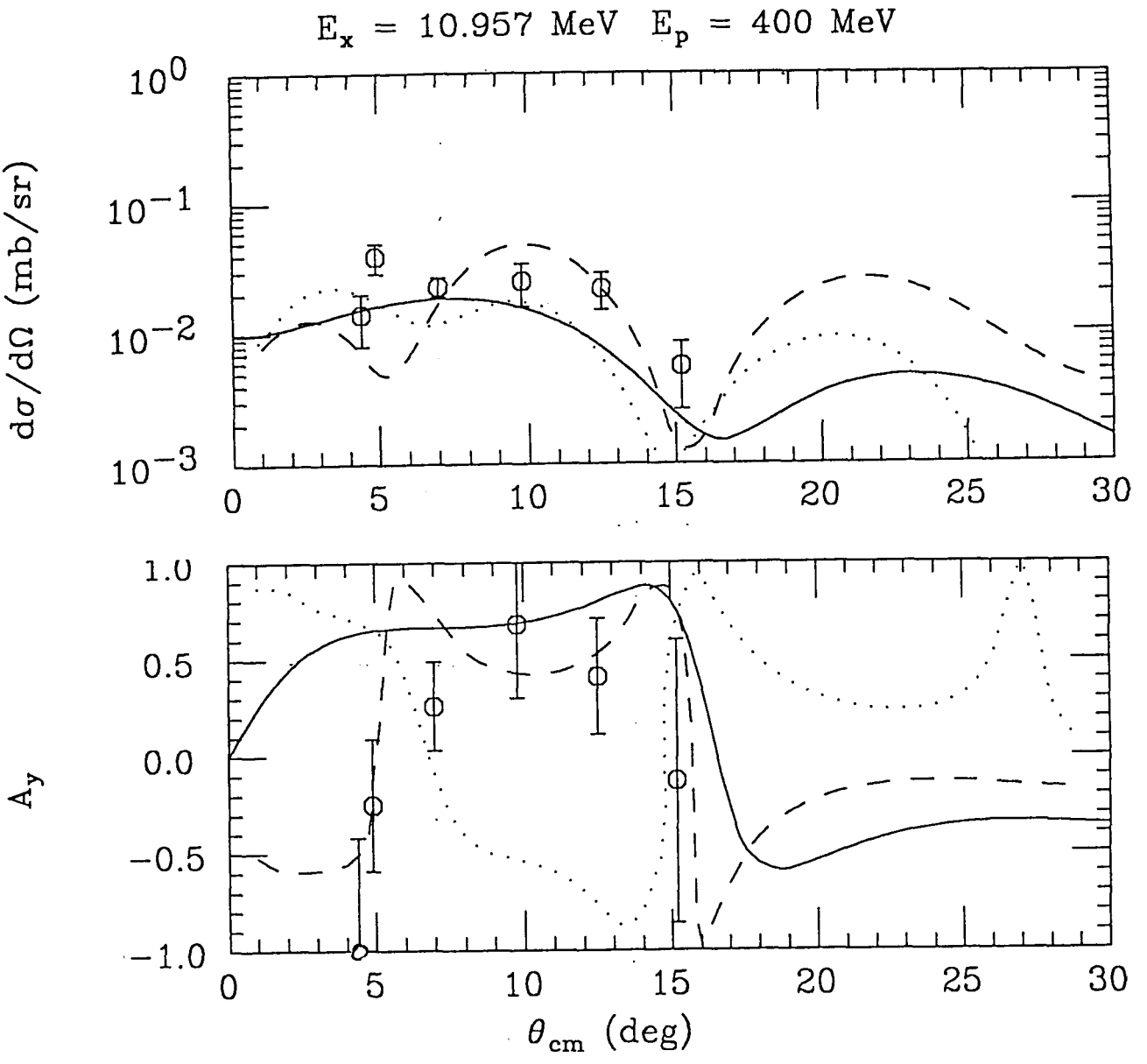

Fig. 2. Experimental and theoretical cross sections and analyzing powers for the excitation of the 10.957 MeV 0^- level of ^{16}O by 400 MeV protons. The data are taken from ref. 4. The solid curve is obtained from a relativistic impulse approximation calculation treating the 0^- state as a pure T=0 level. The dashed cureve is a similar caclulation assuming a pure proton $p^{-1}_{1/2}s_{1/2}$ excitation and the dotted curve uses a pure neutron excitation assumption.

4. **Non-local Correction Factor at Intermediate Energies** P.D. Kunz and TRIUMF collaboration.

The Perey form of the non-locality correction which is based upon the central part of the optical potential and is valid at low energies is not justified at intermediate energies. At these energies the central potential is small and thus gives a much smaller correction than does the equivalent Schrödinger reduction of the Dirac model[1]. In the formulation of the Dirac model the reduction factor for the local equivalent wave function is based upon the Darwin term. In the pseudoscalar theory for the one pion exchange potential (OPEP), this suppression factor is exactly cancelled by the medium corrections[2] for the transition operator. However, in the preferred[3] pseudovector derivative coupling theory for OPEP, the medium corrections are small[4,5] and a suppression factor similar to the Darwin term survives. A close approximation to the factor arising from the Darwin term is

$$f(r) = \exp[\frac{1}{2} w_s(r)], \tag{1}$$

where we can express $w_s(r)$ as,

$$w_s(r) = \ln[(E + mc^2 - V(r) + S(r))/(E + mc^2)]. \tag{2}$$

Here V(r) and S(r) are the vector and scalar potentials, respectively, E is the total energy of the projectile, and the spin-orbit potential is obtained from $w_s(r)$ by

$$V_{so}(r) = -\frac{\hbar^2}{m}\frac{1}{r}\frac{d}{dr} w_s(r). \tag{3}$$

At intermediate energies, optical model potentials which are obtained from fits to experimental data are assumed to be the equivalent Schrödinger potentials arising from the reduction of the Dirac equation to a two-component form. Hence, given the spin-orbit potential $V_{so}(r)$, it is straightforward to reconstruct the non-local factor from Eq. (1) and Eq. (3) by a numerical integration,

$$f(r) = \exp\Big[\frac{1}{2}\frac{m}{\hbar^2}\int_{\infty}^{r} r'\, V_{so}(r')\, dr'\Big].$$

This expression has been included as an option in the distorted wave codes DWUCK4 and DWUCK5 to calculate non-locality corrections in a more suitable way for intermediate energy proton scattering.

1. B.C. Clark, R.L. Mercer and P. Schwandt, Phys. Lett. **122B**, 211 (1983)
2. E.D. Cooper, A.O. Gattone and M.H. Macfarlane, J. Phys. G**9**, L131 (1983)
3. B.D. Serot and J.D. Walecka, *Advances in Nuclear Physics* (Plenum, New York, 1986), Vol. 16, p.4.
4. P.D. Kunz and E. Rost, J. Phys. G**14**, L253 (1988)
5. E.D. Cooper, A.O. Gattone and M.H. Macfarlane, Phys. Lett. **130B**, 359 (1983)

5. **Deuteron Knockout in the $(e, e'd)$ Reaction** P.D. Kunz and H.P. Blok (Vrije Universiteit, Amsterdam)

The $(e, e'd)$ reaction is a very useful way to study nucleon correlations and obtain information about the two-nucleon density function $\rho_2(\mathbf{r_1}, \mathbf{r_2})$. The study of this correlation function is superior to the two nucleon pickup reactions, such as the (p,t) reaction, since the interpretation of the electron reaction is cleaner. The interaction for the electron is known, is relatively weak, and for light nuclei the Coulomb distortion can be neglected. We wish to understand aspects of the correlations can be studied with only one outgoing particle which is the current experimental situation.

One important important issue to be addressed is the amount which higher order processes affect the useful nuclear structure that is to be extracted using this reaction. It is well known that in transfer reactions[1] that second-order terms in the transition amplitude such as sequential pick-up processes are nearly as large as the direct term. This implies that the $(e, e'd)$ reaction can be can be viewed as a knockout of a proton followed by the pickup of a neutron. An equivalent description of such higher order proceeses is to include the knockout of the deuteron via its breakup channels. The role and importance of these two possible mechanisms must be understood before useful information can be extracted from this reaction.

Our model hamiltonian for the $A+2(e, e'd)A$ reaction is given in terms of an electron, a proton and a neutron outside of core A:

$$H = H_A(\xi_i) + K + v_{ep} + v_{pn} + V_e + V_p + V_n, \tag{1}$$

where K is the kinetic energy operator for the three particles, v_{pn} is the inter-nucleon interaction, V_p and V_n are the microscopic interactions of the nucleons with the core, and $H_A(\xi_i)$ is the hamiltonian of the core. The electron is assumed to interact by only the charge component of v_{ep} and V_e, hence the spin degrees of freedom can be suppressed and the electron can be treated as a plane wave in zeroth order. The V_i may contain an imaginary part to take into account absorption from channels that are neglected in our model and may be approximated by a central optical potential U_i.

The wave functions needed for the transition amplitude may be expressed in terms of a set of coupled equations,

$$\begin{aligned}
&(\frac{\hbar^2}{2m}q^2 - \frac{\hbar^2}{2m}\nabla_p^2)\phi_1(\mathbf{r_p}) = 0 \\
&(E_{p,m} - \frac{\hbar^2}{2m_p}\nabla_p^2 - U_p)\chi_{p,m}(\mathbf{r_p}) = \langle \Phi_{A+1,m}(\mathbf{r_n}, \xi_i)|e^{i\mathbf{k_r}\cdot\mathbf{r}}|\Phi_{A+2}(\mathbf{r_p}, \mathbf{r_n}, \xi_i)\rangle \phi_1(\mathbf{r_p}) \\
&(E_d - \frac{\hbar^2}{2m_d}\nabla_R^2 - U_d)\chi_d(\mathbf{R}) = \sum_m \langle \phi_d(\mathbf{r})\Phi_{f,A}(\xi_i)|v_{pn}|\Phi_{A+1,m}(\mathbf{r_n}, \xi_i)\rangle \chi_{p,m}(\mathbf{r_p}),
\end{aligned} \tag{2}$$

where the $\chi_d(\mathbf{R})$ and $\chi_{p,m}(\mathbf{r_p})$ have the boundary conditions of outgoing waves only. The incoming channel describes a fictitious light particle of momentum q which picks up a proton. The proton then propagates in an intermediate channel m and picks up a neutron to form the deuteron in the final state. In setting up these equations the mass and energy of the incoming particle and the Q value for initial step must be chosen so that the kinematics of the intermediate state are described correctly. It is seen that there is no direct term contributing to the reaction in this formulation ("prior form").

Using operator expansions and integrating factor techniques, we can obtain an approximate uncoupled form for the last equation,

$$\begin{aligned}(E_d - \frac{\hbar^2}{2m_d}\nabla_R^2 - U_d)\chi_d(\mathbf{R}) \\ = D_0 \sum_m \frac{1}{1 - R_0^2 A(R)} \langle \Phi_{f,A}(\xi_i) | \Phi_{A+1,m}(\mathbf{r_n}, \xi_i) \rangle \chi_{p,m}(\mathbf{r_p})|_{\mathbf{r_p},\mathbf{r_n}=\mathbf{R}} \\ + D_0 \frac{M}{\hbar^2} \frac{R_0^2}{1 - R_0^2 A(R)} \langle \Phi_{f,A}(\xi_i) | \Phi_{A+2}(\mathbf{r_p}, \mathbf{r_n}, \xi_i) \rangle \phi_1(\mathbf{r_p})|_{\mathbf{r_p},\mathbf{r_n}=\mathbf{R}}.\end{aligned} \tag{3}$$

Here, the finite range corrections contain

$$A(R) = \frac{M}{\hbar^2}[(E_d - U_d) - (E_n - U_n) - (E_p - U_p)]. \tag{4}$$

The first term on the right gives the on-shell finite range correction and the second term gives the off-shell correction. These equations can now be solved using a zero range approximation with first order corrections.

As a test we consider the $^{12}C(e,e'd)^{10}B$ reaction to the 1+ state at 0.72 MeV with an electron momentum transfer of 376 MeV/c and a missing energy of 38 MeV. We show in Fig. 1 the direct term and, for comparison, the sequential transfer term with and without the finite range correction term. The optical model parameters for the proton are those of Schwandt *et al.*[2] and the deuteron potentials are derived from the adiabatic prescription using the parameters of Becchetti and Greenlees[3]. The magnitude for the sequential knockout mechanism gives enhancements of up to 50% in the forward direction and indicates that higher-order processes may be not be negligible. Final assessment of the non-direct effects must await the formulation and calculation of the deuteron breakup state contributions.

1. J. Bang and S. Wollesen, Phys. Lett. **33B**, 396 (1970).
2. P. Schwandt *et al.*, Phys. Rev. **C26**, 55 (1982).
3. F.D. Becchetti and G.W. Greenlees, Phys. Rev. **182**, 1190 (1969).

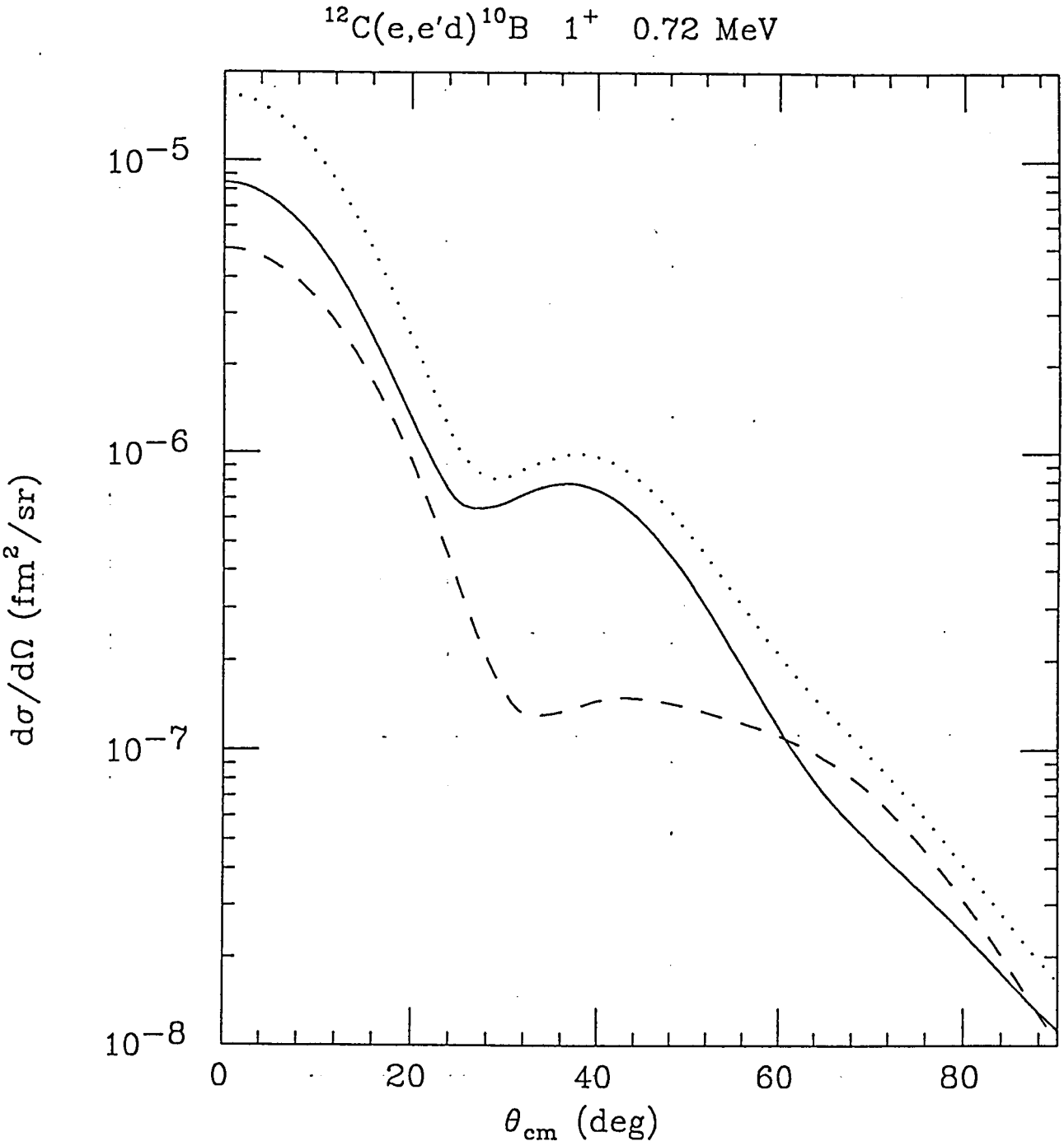

Fig. 1. Differential cross section for the $^{12}C(e,e'd)^{10}B$ reaction at q = 376 MeV/c and for E_m = 38 MeV. The long-dashed curve is the direct reaction and the dotted curve is the sequential term without the off-shell finite range contribution. The solid curve results from the sequential plus off-shell finite range correction.

6. Coulomb-Nuclear Interference in Pion Inelastic Scattering

P.D. Kunz, D.S. Oakley, and C.L. Morris (Los Alamos)

Pion inelastic scattering can give a unique signature of the interference between Coulomb and nuclear forces (CNI) because of the $\Delta_{3,3}$ pion-nucleon scattering resonance at incident pion energies near 180 MeV. Here the Coulomb excitation amplitude is expected to interfere destructively with the π^+-nucleus interaction below the 3,3 resonance and constructively above it (and conversely for π^-). (At resonance, where the π-nucleus interaction is imaginary and the amplitudes add incoherently, we expect CNI to be unimportant.) This CNI phase change is unique to pion scattering; however its effect is only observable in heavy nuclei where Coulomb and pion-nuclear interactions are comparable.

Another significant feature of pion-nucleus scattering near the 3-3 resonance (T_π=100-300 MeV) is that at these energies the π^- is more sensitive to the neutrons in the nucleus while the π^+ is more sensitive to the protons. In these types of measurements, neutron and proton multipole matrix elements M_n and M_p, whose squares scale with the π^- and π^+ cross sections, can be extracted from simultaneous fits to the π^- and π^+ data.[1] For strong collective states the agreement between M_p values extracted from electron scattering, pion scattering and gamma de-excitations is remarkably good.[2] In addition, the M_n and M_p values measured from pion scattering for the first 2^+ states in light T=1 nuclei compare well with their mirror-nuclei counterparts.[3] Consequently we believe that pion scattering can be a reliable tool in identifying effects such as CNI.

In order to investigate the effects of CNI on pion scattering we have performed calculations that employ the distorted-wave impulse approximation (DWIA) both with and without Coulomb excitation included. Here we use the code DWPI[4] with a standard Kisslinger potential including a -28 MeV empirical energy shift and collective-model (Tassie) form factors. The collective-model is characterized by deformation parameters, β_n and β_p, which are proportional to the matrix elements M_n and M_p. In these calculations Coulomb terms, derived from a uniform nuclear matter density approximation, were incorporated along with nuclear form factors[4]. The resulting calculations for the ^{208}Pb$(\pi,\pi')^{208}$Pb interaction show the expected behavior, i.e., the effect of the Coulomb excitation contribution is to change the peak of the differential cross section by about 10-20% for the π^+ at the energies 120 and 250 MeV and by 5-10% for the π^-, with the respective phase changes as shown in Fig. 1. For the calculations at T_π=180 MeV the Coulomb effects are indeed seen to be negligible. If we perform the same calculation for a smaller nucleus such as ^{40}Ca, however, the effect is too small to observe at all of these energies.

The resulting angular distribution shapes were accurately reproduced by the full DWPI calculations. With no Coulomb excitation, however, the magnitudes of the cross sections could not be reproduced without energy variation of the deformation parameters. These deformation parameters are not expected to vary with energy and no such variation has been observed from pion scattering to

low-lying collective states of light and medium mass nuclei. In conclusion, we have found that Coulomb excitation of the low-lying collective states in ^{208}Pb is significant in pion inelastic scattering above and below the 3-3 resonance. Inclusion of Coulomb excitation gives, within error, energy-independent matrix-element ratios of M_n/M_p for the first 2^+, 3^-, and 4^+ states in ^{208}Pb.

1. C. L. Morris, Phys. Rev. **C13**, 1755 (1976).
2. C. L. Morris *et al.* Phys. Rev. **C 35**, 1388 (1987).
3. D. S. Oakley and H. T. Fortune, Phys. Rev. **C37** 1126 (1988).
4. R. A. Eisenstein and G. A. Miller, Comp. Phys. Comm. **11**, 95 (1976).

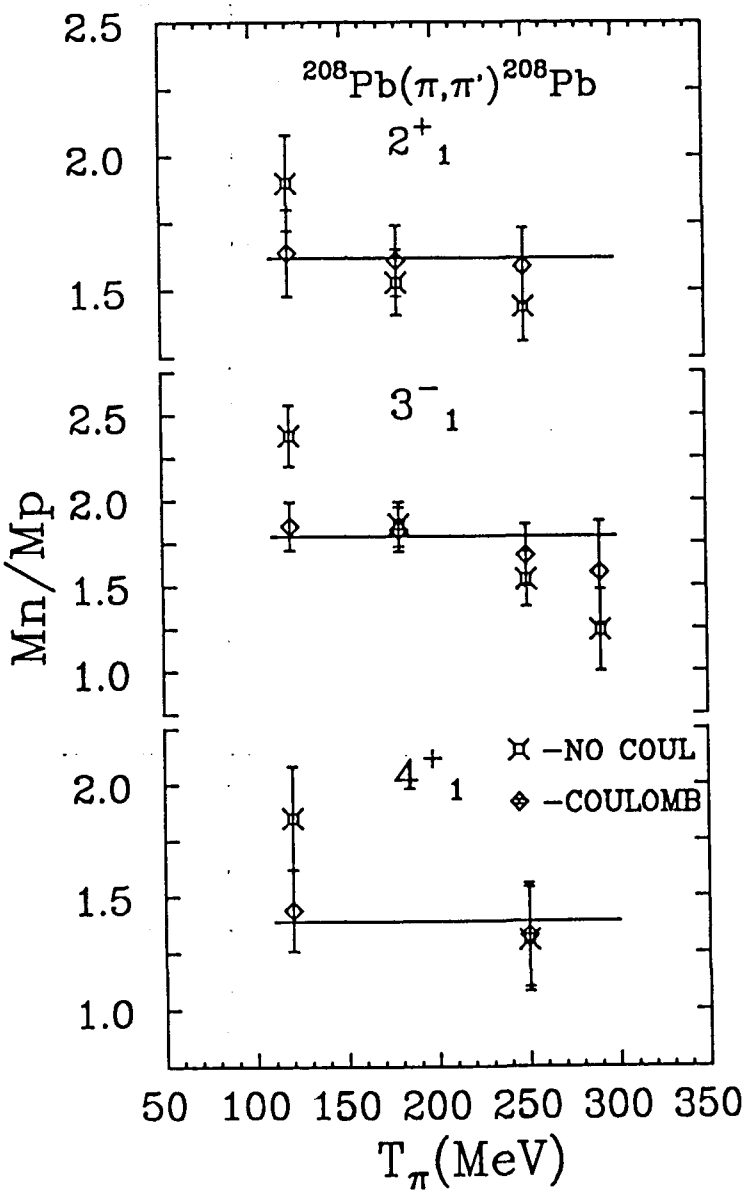

Fig. 1. Comparisons of L=3 DWPI ^{208}Pb$(\pi,\pi')^{208}$Pb Tassie-model calculations with (solid lines) and without (dashed lines) Coulomb excitations included. These particular calculations give matrix element values of M_n=1194 e fm^3 and M_p=777 e fm^3 yielding a hydrodynamic ratio of M_n/M_p=1.54.

7. Instability of Nuclear Matter in a Relativistic Mean Field Model

C. E. Price, J. R. Shepard and J. A. McNeil

The relativistic mean field theory[1], QHD-1, has been very successful in describing the ground state properties of finite nuclei throughout the periodic table. One of the underlying strengths of this model is that there are very few free parameters and that these parameters are determined at the outset by insisting that the model reproduce the empirically determined saturation properties of infinite nuclear matter. Implicit in this method of fixing the model parameters is the assumption that the ground state of infinite nuclear matter is spatially uniform and may be described in terms of a filled Fermi sea of plane wave states. In 1960, Overhauser[2] demonstrated in a one-dimensional calculation that the lowest energy state of nuclear matter was not necessarily uniform. He found that in the limit of very short range interactions the nuclear matter ground state contained an oscillatory structure with a period given by the Fermi momentum. In this work, we have investigated the possibility that the Overhauser effect is present in the relativistic mean field model in three dimensions.

One simple way to demonstrate the instability of the uniform state of nuclear matter is to use the random phase approximation (RPA) to calculate the excitation energies of the low-lying excited states of the uniform system. It is a general property of the RPA that all of the excited state energies are real. If the RPA ground state is not the lowest energy state of the system then at least one of the RPA energies will be imaginary. In Fig. 1 the shaded area shows the region in which the uniform state is not the lowest energy state of the system. This instability is sensitive to the range of the scalar interaction (which is given by the scalar mass) and to the momentum transfer, q, which determines the period of the oscillatory component of the non-uniform state. The lowest scalar mass for which the instability appears is 575 MeV and is associated with a momentum transfer of roughly $1.6k_F$, where k_F is the Fermi momentum. The value for the scalar mass is very close to the values that are typically used in relativistic models.

In order to study the details of the periodic state, we need a self-consistent calculation of the nuclear matter wave functions and mean fields that does not rely on the assumption that infinite nuclear matter is uniform. This is acheived by allowing the mean fields to contain a spatial variation (assuming cubic symmetry) with a period given by $q = 1.6k_F$, and by describing the nuclear wave functions as a superposition of many plane wave states with different momenta. In Fig. 2 we show a cross section of the three dimensional density for nuclear matter in the periodic state. Each of the high density regions contains two protons and two neutrons, so in the non-uniform state nuclear matter crystallizes into alpha particles on a cubic lattice. In a spherically symmetric system this alpha particle clustering would lead to radial density oscillations of roughly the same period.

Since there is a large range of scalar masses for which the nuclear matter ground state is not uniform it is inappropriate to fix the model parameters to uniform nuclear matter properties. If the parameters are readjusted to reproduce the empirical saturation data within the periodic system, we find that the system is slightly less attractive and that the nuclear compressibility is somewhat

reduced. Each of these effects may help to solve a problem within the relativistic model. In RPA calculations of the excited states of finite nuclei[3] the ground state of ^{40}Ca is unstable. This instability is typically avoided by reducing the attractive scalar coupling by about two percent. This reduction is comparable to the reduction of the attraction in the periodic state. One of the most serious problems of the relativistic model is that the predicted nuclear compressibility is too large by a factor of two. While the reduction of the compressibility in the periodic state is not sufficient to eliminate this problem, it is a step in the right direction.

Finally, in calculations of finite nuclei within the relativistic model, the radial density shows an oscillation with a period that is consistent with the alpha clustering described above and the magnitude of the oscillation is very sensitive to the value of the scalar mass. Furthermore, the nuclear charge density data also show a periodic component of roughly the same period. This indicates that the Overhauser effect[2] is certainly present within the relativistic model and that this is not in disagreement with the data. The ultimate conclusion of this work is that infinite nuclear matter cannot be described simply in terms of plane waves and that it is therefore important to make use of the properties of real finite nuclei in order to adjust the model parameters.

1. B.D. Serot and J.D. Walecka, Adv. Nucl. Phys. **16**, 1 (1986)
2. A.W. Overhauser Phys. Rev. Lett. **4**, 415 (1960)
3. J.R. Shepard E. Rost and J.A. McNeil, Phys. Rev. **C** to be published.

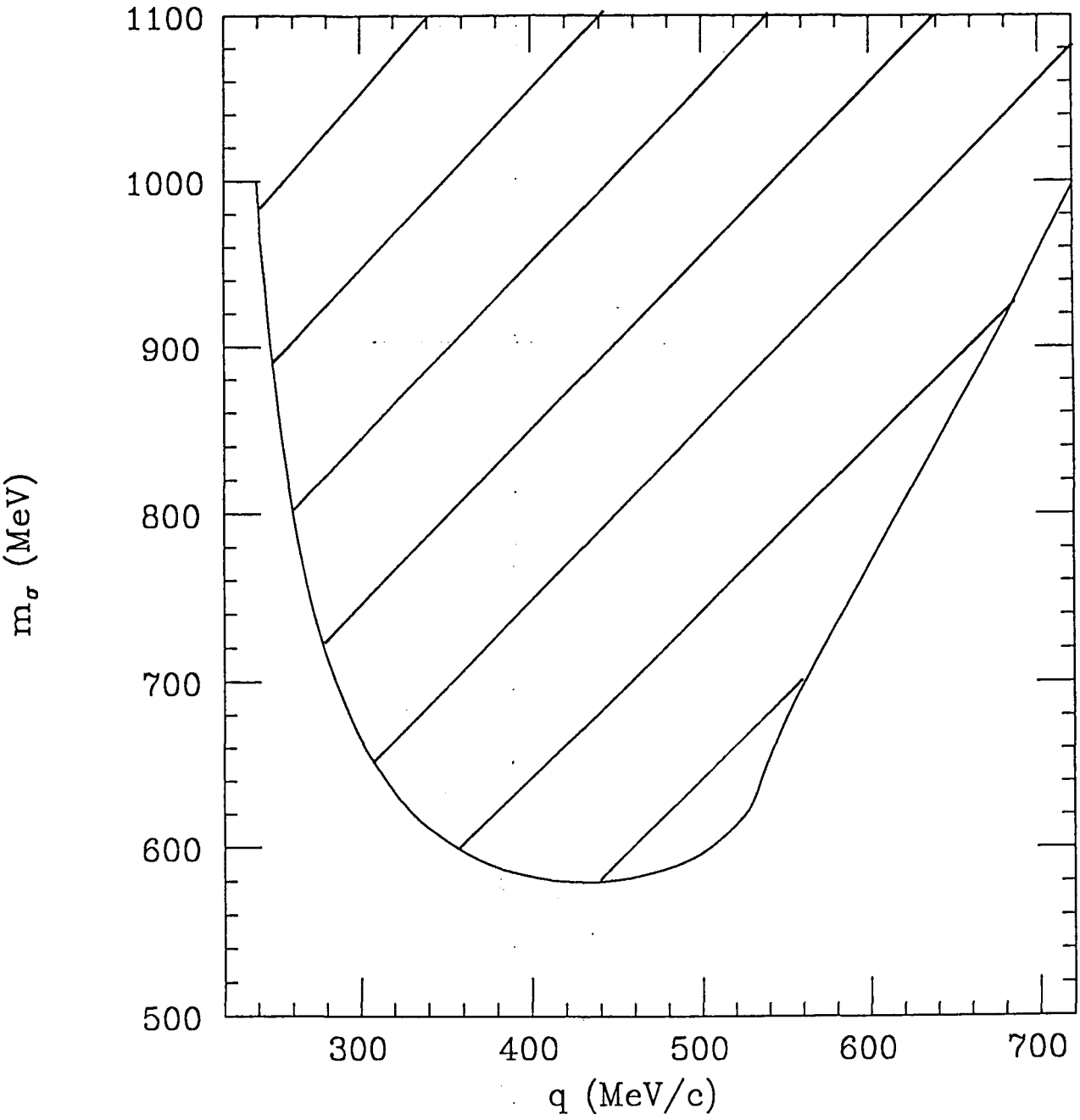

Fig. 1. Region of instability of the uniform state of infinite nuclear matter as a function of the scalar mass and the momentum transfer.

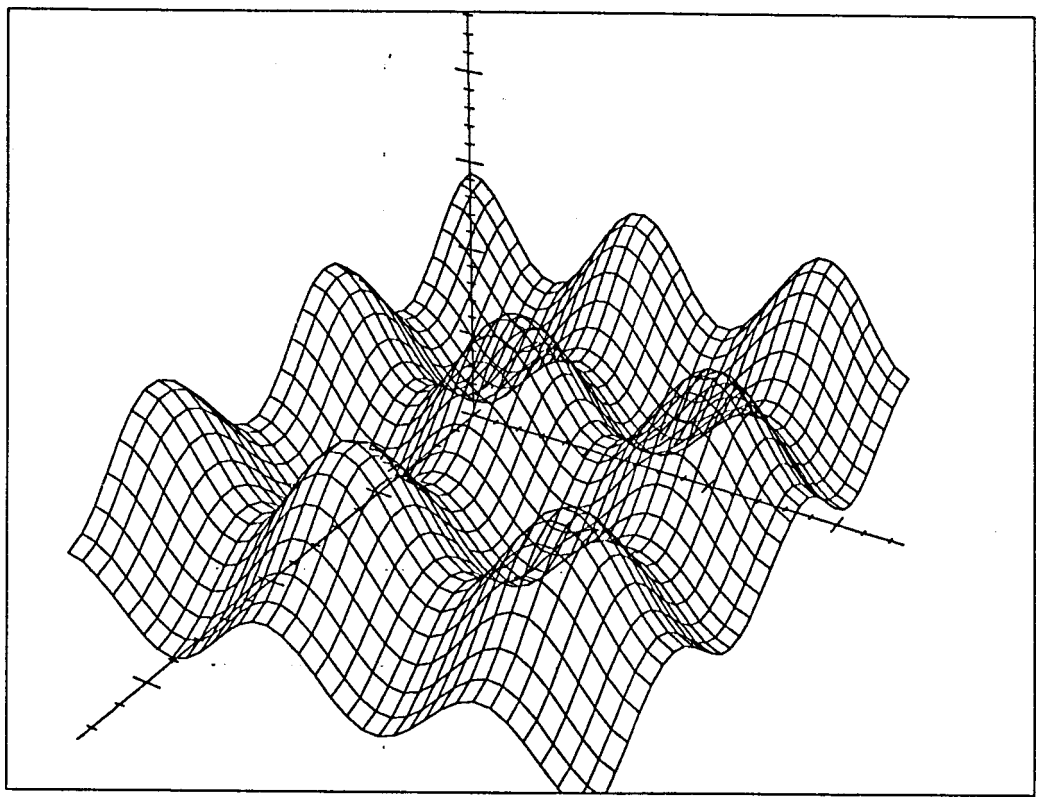

Fig. 2. Two dimensional cross section of the density of nuclear matter in the periodic state.

8. Spin-Flip Cross Sections for $^{13}C(\vec{p},\vec{n})^{13}N$(g.s.) at 500 MeV J. R. Shepard and L. Ray (Texas)

Charge exchange reactions at intermediate energies are an emerging, important new field of research in nuclear physics[1]. We have analyzed the longitudinal and transverse spin-flip cross sections and the projectile no-spin-flip cross section for the particular reactions $^{13}C(\vec{p},\vec{n})^{13}N$(g.s.) and $^{15}N(\vec{p},\vec{n})^{15}O$(g.s.) and have presented an optimal procedure for analyzing such data in the future. The results and the predicted sensitivities are based on the relativistic distorted wave approximation of the RIA - Dirac equation model, the latter of which has had considerable success fitting proton elastic scattering data from even-even target nuclei at intermediate energies. This model provides a description of existing intermediate energy charge exchange differential cross section and analyzing power data which is, in general, superior to that obtained with nonrelativistic DWIA models. It is, however, deficient with respect to recent 500 MeV $^{15}N(\vec{p},n)$ analyzing power data[2] and it is this fact which primarily motivated the present work.

We have shown that the optimum method for analyzing isobaric analogue (p,n) reaction data at intermediate energies from light, odd target nuclei and for critically testing and (hopefully) improving the relativistic DWIA model consists of the following steps:

(1) The quantity[3] σS_{FP}^{T} can be used to test and constrain the Lorentz invariant, isovector-tensor amplitude together with the valence nucleon upper component wave function.

(2) The data for σS_{FP}^{L} can be subsequently analyzed with respect to the isovector- pseudoscalar invariant and the lower component of the valence nucleon wave function.

(3) Data for σ_o at forward angles can be used to study the Fermi transition amplitude, A_F.

(4) If (p,n) data for polarized targets are made available, then empirical constraints on the Fermi - GT interferences can be imposed.

The reaction model which fits σS_{FP}^{T}, σS_{FP}^{L}, and σ_o will not necessarily reproduce all other measured observables since a complete amplitude determination cannot be carried out based on the limited subset of data available with unpolarized targets. The calculations must continue to be compared with the differential cross section, analyzing power and polarization transfer data directly in order to further test and constrain the Fermi portion of the transition amplitude, the tensor and pseudoscalar contributions to the GT transition amplitude, and the valence nucleon wave function.

Analyses of the combination of polarization transfer measurements in conjunction with differential cross section and analyzing power data for these (p,n) reactions may provide a rich new source of information with which to further test both relativistic and nonrelativistic reaction models. These results may also

enable information to be obtained regarding the inadequacies of the relativistic DWIA model for the (p,n) channel. Eventually analyses of such data may be used to constrain the poorly known isovector components of the intermediate energy NN effective interaction, to further study the effects of the nuclear medium, and to differentiate nonrelativistic and relativistic models of nuclear structure.

A paper describing the details of this work has been accepted for publication in Physical Review C.

1. see, Los Alamos Meson Physics experimental proposals 1041, 1061, and 1062.
2. D.Ciskowski, *et al.*, B.A.P.S. **33**, 1583 (1988); D.Ciskowski, Ph.D. thesis, University of Texas (1989); T.N.Taddeucci, private communication.
3. This quantity is the spin-flip cross section as defined in L.Ray *et al.*, Phys. Rev. **C37**, 1169 (1988).

9. **Vacuum Fluctuation Effects in Open-Shell Nuclei within the Relativistic $\sigma - \omega$ Model** C. E. Price and R. J. Furnstahl (University of Maryland)

Relativistic mean-field models have been very successful in describing the equilibrium properties of spherical and axially deformed nuclei, including rms radii, charge densities, quadrupole moments and nuclear shell structure[1]. Recently, this success has been extended to magnetic moments and other properties of more general open-shell nuclei having at least one unpaired proton or neutron[2].

In this earlier work we investigated the importance of the vacuum fluctuation effects for the magnetic moments and elastic magnetic form factors of various nuclei near closed shells. The results for the isoscalar magnetic moments of several light mass systems are summarized in the following table.

A	Schmidt	Valence	MFT	RHA	Exp.
11	0.940	1.126	0.963	0.960	0.862
13	0.187	0.307	0.182	0.172	0.190
15	0.187	0.343	0.199	0.191	0.218
17	1.440	1.570	1.426	1.440	1.414
39	0.636	1.012	0.660	0.650	0.706
41	1.940	2.253	1.942	1.950	1.918

Clearly both the mean-field theory (MFT) results and relativistic Hartree (RHA) results (which include the vacuum) are in good agreement with the experimental data and with the non-relativistic Schmidt values. These results also indicate that the vacuum fluctuations play only a rather small role in determining the magnetic moments of nuclei near closed shells. In Fig. 1, we show the elastic magnetic form factor for ^{209}Bi. For all but the lowest values of the momentum transfer, q, the vacuum effects (RHA) significantly reduce the form factor. Since the mean field result is significantly enhanced, this reduction (due to the vacuum fluctuations) improves the agreement with the experimental results. However, in this calculation the vacuum fluctuations were included in the local density approximation (LDA), which is probably inadequate for open-shell systems where the spatial variation (due to the increased deformations) is more pronounced. Wasson[3] has derived a derivative expansion (DE) for the vacuum fluctuation effects which includes the leading order corrections to the LDA.

In the current work, we have included these derivative corrections in our calculations for open-shell nuclei. The dotted line in Fig. 1 shows the results for the elastic magnetic form factor of ^{209}Bi. Clearly, the local density and derivative expansion results are very similar. There is a slight reduction from the LDA form factor, but the change is small enough that it should not affect any qualitative

LDA and DE results for the magnetic moments for the closed shell ± 1 systems shown in the table above. These results cannot be taken as an absolute indication that the derivative corrections may be ignored. We expect that the derivative corrections will be increasingly important for nuclei that are farther from the closed shells. More detailed results for a broader range of nuclei are forthcoming.

1. B.D. Serot and J.D. Walecka, Adv. Nucl. Phys. **16**, 1 (1986); C.E. Price and G.E. Walker, Phys. Rev. **C36**, 354 (1987); R.J. Furnstahl, C.E. Price and G.E. Walker, Phys. Rev. **C36**, 2590, (1987)
2. R.J. Furnstahl and C.E. Price, to be published in Phys. Rev. **C**
3. D.A. Wasson, "Effect of Vacuum Polarization on Nuclear Structure", preprint, (1988)

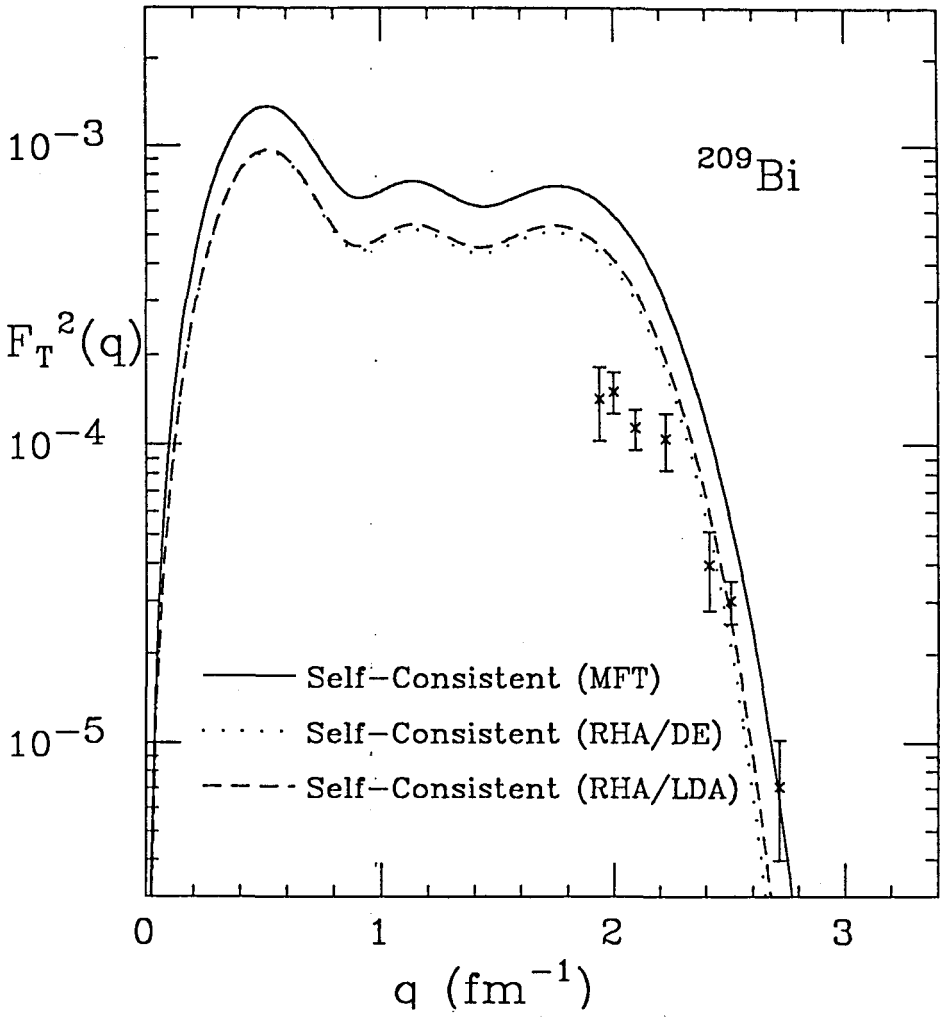

Fig. 1. Elastic magnetic form factor for ^{209}Bi. The solid line shows the usual mean-field results with no vacuum fluctuations included. The results shown by the dashed curve include the vacuum effects in the local density approximation and those shown by the dotted curve include the additional derivative corrections.

10. $^3P_0$ and $^3S_1$ Contributions to $\bar{p}p \rightarrow \bar{\Lambda}\Lambda$ P.D. Kunz and Univ. Washington collaboration

We have proposed[1] a quark model for $\bar{N}N$ annihilation which consists of a linear superposition of the so-called $^3P_0$ (scalar) and $^3S_1$ (vector) models. We have argued that this approach is more consistent with QCD and the analogous NN system than the use of either model alone. Recent precise measurements[2] of the $\bar{p}p \rightarrow \bar{\Lambda}\Lambda$ reaction by the PS185 collaboration at LEAR provide a test of this model. An advantage of strange baryon production is the polarization information that can be obtained due to their weak decays. Spin effects are known to be more sensitive to details of the reaction mechanism.

One possible description of the $\bar{p}p \rightarrow \bar{\Lambda}\Lambda$ reaction is that of K- and K*-meson exchange. Such exchanges are of short range, at distances for which quark effects might be expected to play a role. Therefore alternative descriptions[3] based on constituent quark dynamics have been developed. These models are based on either the $^3P_0$ model, in which a $\bar{u}u$ pair annihilation into the vacuum is followed by an $\bar{s}s$ creation, or the $^3S_1$ model, in which a virtual vector quantum is exchanged. We have proposed that the correct description for $\bar{N}N$ annihilation consists of a superposition of the $^3P_0$ and $^3S_1$ mechanisms, since the former can arise from the confining scalar force and the latter describes the vector quantum exchange expected in the $\bar{N}N$ interaction.

We used the same distorting potentials for $\bar{N}N$ and $\bar{\Lambda}\Lambda$ as Kohno and Weise.[3] For $\bar{N}N$ the real part of the potential is determined by G-parity transformation of the long-range part of a realistic one-boson exchange potential, with a smooth extrapolation to $r = 0$. The imaginary part, which represents annihilation, is of Gaussian form and is adjusted to produce good fits to experimental data. For the real part of the $\bar{\Lambda}\Lambda$ interaction Kohno and Weise use the isoscalar boson exchanges of the real part of the $\bar{N}N$ potential. The annihilation term is taken to be of the same form as that for the $\bar{N}N$, but with a strength adjusted to fit total cross section data.

Our results for differential cross sections and polarization at 1.5075 GeV/c and 1.564 GeV/c are shown in Figs. 1 and 2. Our best fits (minimum χ^2) to the experimental data[2] are shown for the scalar model alone, the vector model alone, and the superposition. For the scalar and vector models alone we searched on the oscillator radius r_0; for our superposition we searched on r_0 and the ratio g_v/g_s. As seen in Fig. 1, at the lower momentum the differential cross section can be fit reasonably well by either term alone or the superposition, but a much better fit to the polarization data is obtained by using the combined terms, with $r_0 = .89$ fm and $g_v/g_s = -.19$. At the higher momentum shown in Fig. 2 the vector term alone fits the differential cross section better than the scalar, but neither fits the polarization well. An improved fit is found by using the linear combination, with $g_s/g_v = -.42$. One characteristic of the polarization data that we, as well as other authors, have found difficult to fit is the crossing point, i.e. the angle at which the polarization changes sign.

We have shown that the best fit to $\bar{p}p \rightarrow \bar{\Lambda}\Lambda$ at two energies occurs for

an interference between scalar and vector mechanisms, rather than for either term alone. The sensitivity of our results to the parameters of the $\bar{\Lambda}\Lambda$ potential indicates that the $\bar{p}p \rightarrow \bar{\Lambda}\Lambda$ reaction may be a source of information on the $\bar{\Lambda}\Lambda$ interaction.

1. M.A. Alberg, E.M. Henley, and L. Wilets, Z. Phys.**A331**, 207 (1988)
2. P.D. Barnes *et al.*, Phys. Lett. **B189**, 249 (1987); *Physics at LEAR with low energy antiprotons*, eds. C. Amsler *et al.* (Harwood, London, 1988) pp. 347-352; K. Kilian, Nucl. Phys.**A479** (1988) 425c
3. see, *e.g.*,M. Kohno and W. Weise, Phys. Lett. **B179**, 15 (1986)

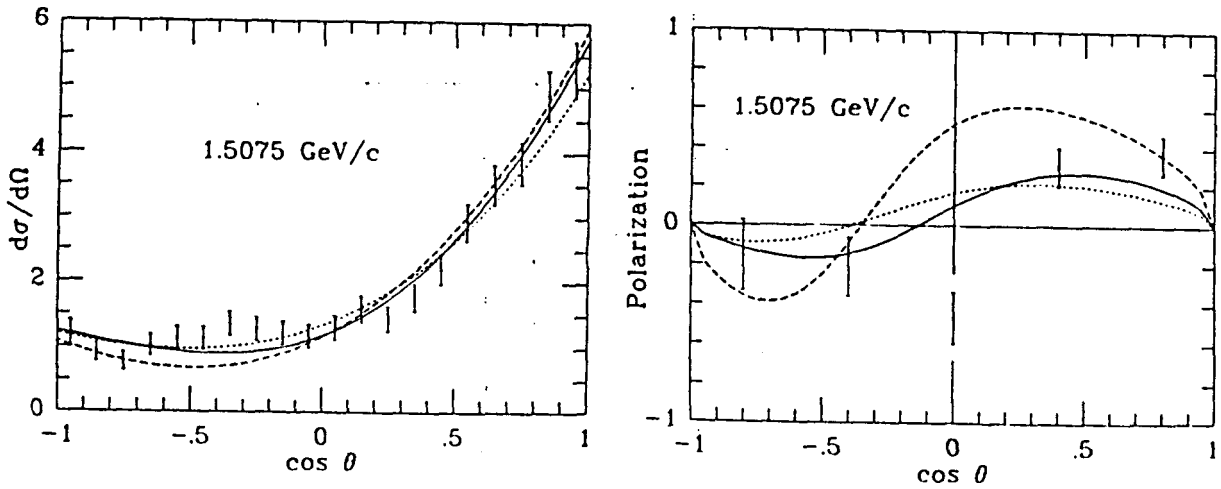

Fig. 1. Differential cross section and polarization for $\bar{p}$ lab momentum of 1.5075 GeV/c. The long-dashed curve is the vector contribution (for r_0 = .65 fm) and the short-dashed curve is the scalar contribution (for r_0 = .56 fm). The solid curves are the result of a linear combination ($I_v + I_s$), with g_v = -.19 g_s and r_0 = .89 fm.

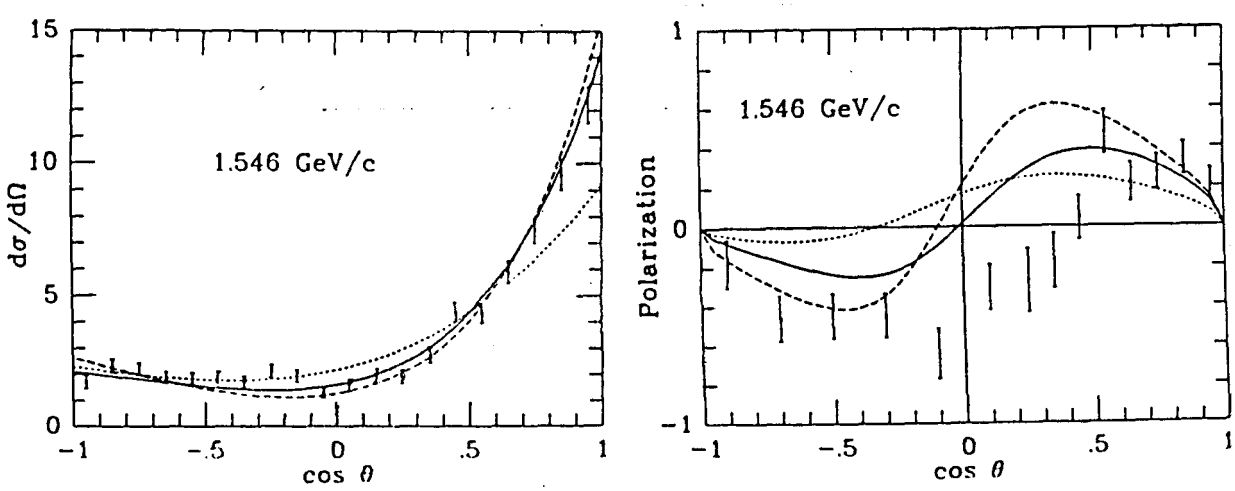

Fig. 2. Differential cross section and polarization for $\bar{p}$ lab momentum of 1.564 GeV/c. The long-dashed curve is the vector contribution (for r_0 = .82 fm) and the short-dashed curve is the scalar contribution (for r_0 = .62 fm). The solid curves are the result of a linear combination ($I_v + I_s$) with g_v = -.42g_s and r_0 = .98 fm.

B PUBLICATIONS AND REPORTS—October 1, 1988 to August 1, 1989

1. Published Articles

1. Relativistic Suppression Factors in (p,d) Reaction Calculations, P. D. Kunz and E. Rost, Jour. Phys. G. **14**, L253 (1988)
2. Spin-Dependent Observables for the ^{12}C(p,p'γ) Reaction at 400 MeV, K. H. Hicks, R. Abegg, K. P. Jackson, C. A. Miller, S. Yen, A. Cellar, O. Hausser, R. G. Jeppesen, A. Trudel, M. Vetterli, R. S. Henderson, M. W. Hill, N. S. P. King, G. L. Morgan, M. A. Kovash, and J. R. Shepard, Phys. Rev. Lett.
3. Cross sections and Analyzing Power Measurements for the (p,d) Reaction on ^{16}O and ^{40}Ca at 200 MeV, P.D. Kunz, R. Abegg, D. Hutcheon, C.A. Miller, L. Antonuk, J.M. Cameron, G. Gaillard, J.M. Greben, P. Kitching, R.P. Liljestrand, W.J. McDonald, W.C. Olsen, G.M. Stinson and J. Tinsley, Physical Review **C 39**, 65 (1989).
4. Angular Momentum Selectivity in Transfer Reactions with Heavy Deformed Nuclei, H. Esbensen, S. Landowne and C. Price, Nucl. Phys. **A491**, 147 (1989).

2. Articles Accepted or Submitted for Publication

1. Non-Spectral Dirac RPA for Finite Nuclei, J.R. Shepard, E. Rost and J.A. McNeil, accepted by Phys. Rev. C.
2. Finite Nucleus Dirac Mean Field Theory and RPA Using Finite B-Splines, J.A. McNeil, R.J. Furnstahl, E. Rost and J.R. Shepard, accepted by Phys. Rev. C.
3. Spin Flip Cross Sections for ^{13}C(p,n)^{13}N(g.s.) at 500 MeV, L. Ray and J.R. Shepard, accepted by Phys. Rev. C.
4. Relativistic Mean Field Theory for Nuclei, A.R. Bodmer and C.E. Price, accepted by Nucl. Phys. A.
5. Dirac RPA Analysis of the Inelastic Scattering of 500 MeV Protons from ^{40}Ca, E. Rost and J.R. Shepard, submitted to Phys. Rev. C.
6. Correlation Observables in (p,p',γ) Reactions, J. Piekarewicz, E. Rost and J.R. Shepard, submitted to Phys. Rev. C.
7. Coulomb-Nuclear Interference in Pion Inelastic Scattering, P.D. Kunz, D.S. Oakley and C.L. Morris, submitted to Phys. Rev. C.

3. Invited and Contributed Papers

1. Density Modulations in Relativistic Mean-Field Calculations of Nuclear Matter and Finite Nuclei, C.E. Price, J.R. Shepard, S. Tosa and J.A. McNeil, B.A.P.S. **36**, 1246 (1989)
2. Dirac RPA Correlations for Ground States of Finite Nuclei, J.A. McNeil, C.E. Price and J.R. Shepard, B.A.P.S. **36**, 1247 (1989)
3. $^3P_0$ and $^3S_0$ Contributions to $\bar{p}p \rightarrow \bar{\Lambda}\Lambda$, M.A. Alberg, E.M. Henley, L. Wilets and P.D. Kunz, IUPAP Conference on Few Body Problems in Physics, Vancouver, B.C., Canada, July, 1989.
4. Systematics of Light Nuclei in a Relativistic Model, C.E. Price, in *Relativistic Nuclear Many-Body Physics* (World Scientific, 1989).
5. A Relativistic Description of Deformed Nuclei, R.J. Furnstahl and C.E. Price, in *Spin Observables of Nuclear Probes* (Plenum, 1989).

C. PERSONNEL February 1, 1989 to January 31, 1990

1. **Academic and Scientific**

P.D. Kunz	Professor
E. Rost	Professor
J.R. Shepard	Associate Professor
C.E. Price	Research Associate (since Sept, 1988)
J.A. McNeil	Colo. School of Mines (separate funding)

2. **Research Assistants**

T. Morse

T. Ferree

3. **Summer Visitors**

J. Piekarewicz	Indiana University
R. Furnstahl	University of Maryland
K. Wehrberger	Indiana University
N. Auerbach	Tel Aviv University
L. Ray	University of Texas